Combinatorial and Geometric Properties of Planar Laman Graphs

Stephen Kobourov[1⋆], Torsten Ueckerdt[2⋆⋆], and Kevin Verbeek[3⋆⋆⋆]

[1] Department of Computer Science, University of Arizona
[2] Department of Applied Mathematics, Charles University
[3] Department of Mathematics and Computer Science, TU Eindhoven
kobourov@cs.arizona.edu torsten@kam.mff.cuni.cz k.a.b.verbeek@tue.nl

Abstract. Laman graphs naturally arise in structural mechanics and rigidity theory. Specifically, they characterize minimally rigid planar bar-and-joint systems which are frequently needed in robotics, as well as in molecular chemistry and polymer physics. We introduce three new combinatorial structures for planar Laman graphs: angular structures, angle labelings, and edge labelings. The latter two structures are related to Schnyder realizers for maximally planar graphs. We prove that planar Laman graphs are exactly the class of graphs that have an angular structure that is a tree, called *angular tree*, and that every angular tree has a corresponding angle labeling and edge labeling.

Using a combination of these powerful combinatorial structures, we show that every planar Laman graph has an L-contact representation, that is, planar Laman graphs are contact graphs of axis-aligned L-shapes. Moreover, we show that planar Laman graphs and their subgraphs are the only graphs that can be represented this way.

We present efficient algorithms that compute, for every planar Laman graph G, an angular tree, angle labeling, edge labeling, and finally an L-contact representation of G. The overall running time is $\mathcal{O}(n^2)$, where n is the number of vertices of G, and the L-contact representation is realized on the $n \times n$ grid.

⋆ Research supported in part by NSF grants CCF-0545743 and CCF-1115971.
⋆⋆ Research was supported by GraDR EUROGIGA project No. GIG/11/E023.
⋆⋆⋆ Research was supported by the Netherlands Organisation for Scientific Research (NWO) under project no. 639.022.707.

1 Introduction

A *contact graph* is a graph whose vertices are represented by geometric objects (like curves, line segments, or polygons), and edges correspond to two objects touching in some specified fashion. There is a large body of work about representing planar graphs as contact graphs. An early result is Koebe's 1936 theorem [17] that all planar graphs can be represented by touching disks.

In the late 1990's Schnyder showed that maximally planar graphs contain rich combinatorial structure [21]. With an angle labeling and a corresponding edge labeling, Schnyder shows that maximally planar graphs can be decomposed into three edge disjoint spanning trees. This combinatorial structure can be transformed into a geometric structure to produce a straight-line crossing-free planar drawing of the graph with vertex coordinates on the integer grid. Later, de Fraysseix *et al.* [10] show how to use the combinatorial structure to produce a representation of planar graphs as T-contact graphs (vertices are axis-aligned T's and edges correspond to point contact between T's) and triangle contact graphs.

We study the class of *planar Laman graphs* and show that we can find similarly powerful combinatorial structures. In particular, we show that every planar Laman graph G contains an *angular structure*—a graph on the vertices and faces of G with certain degree restrictions—that is also a tree and hence called an *angular tree*. We also show that every angular tree has a corresponding *angle labeling* and *edge labeling*, which can be thought of as a special Schnyder realizer [21]. Using a combination of these combinatorial structures we show that planar Laman graphs are *L-contact graphs*, graphs that can be represented as the contacts of axis-aligned non-degenerate L's (where the vertices correspond to the L's and the edges correspond to non-degenerate point contacts between the corresponding L's). As a by-product of our approach we obtain a new characterization of planar Laman graphs: a planar graph is a Laman graph if and only if it admits an angular tree. The L-contact representation can be computed in $\mathcal{O}(n^2)$ time and realized on the $n \times n$ grid, where n is the number of vertices of G.

Related Work. Koebe's theorem [17] is an early example of point-contact representation and shows that a planar graph can be represented by touching disks. Any planar graph also has a contact representation where all the vertices are represented by triangles in 2D [10], or even cubes in 3D [12].

Planar bipartite graphs can be represented by axis-aligned segment contacts [4, 9, 19]. Triangle-free planar graphs can be represented via contacts of segments with only three slopes [6]. Furthermore, every 4-connected 3-colorable planar graph and every 4-colored planar graph without an induced C_4 using four colors can be represented as the contact graph of segments [8]. More generally, planar Laman graphs can be represented with contacts of segments with arbitrary number of slopes and every contact graph of segments is a subgraph of a planar Laman graph [1].

The class of planar Laman graphs is of interest due to the fact that it contains several large classes of planar graphs (e.g., series-parallel graphs, outer-planar graphs, planar 2-trees). Laman graphs are also of interest in structural mechanics, robotics, chemistry and physics, due to their connection to rigidity theory, which dates back to the 1970's [18]. A system of fixed-length bars and flexible joints connecting them is minimally rigid if it becomes flexible once any bar is removed; planar Laman graphs correspond to rigid planar bar-and-joint systems [15, 16].

While Schnyder realizers were defined for maximally planar graphs [20, 21], the notion generalizes to 3-connected planar graphs [11]. Fusy's transversal structures [14] for irreducible triangulations of the 4-gon also provide combinatorial structure that can be used to obtain geometric results. Both concepts are closely related to certain angle labelings. Angle labelings of quadrangulations and plane Laman graphs have been considered before [13]. However, for planar Laman graphs the labeling does not have the desired Schnyder-like properties. In contrast, the labelings presented in this paper do have these properties.

Results and Organization. In Section 2 we introduce three combinatorial structures for planar Laman graphs. We first show that planar Laman graphs admit an angular tree. Next, we use this angular tree to obtain a corresponding angle labeling and edge labeling. In Section 3 we use a combination of these combinatorial structures to show that planar Laman graphs are L-contact graphs. We then describe an algorithm to compute the L-contact representation of a planar Laman graph G in $\mathcal{O}(n^2)$ time on the $n \times n$ grid. The running time of our algorithm is dominated by the computation of an angular tree of G. Given an angular tree, the algorithm runs in $\mathcal{O}(n)$ time. Appendix A contains a detailed example illustrating the constructive algorithm. Proofs omitted due to space restrictions can be found in Appendix C.

2 Combinatorial Structures for Planar Laman Graphs

Consider a graph $G = (V, E)$. For a subset of vertices $W \subseteq V$, let $G(W)$ be the subgraph of G induced by W, and let $E(W)$ be the set of edges of $G(W)$.

Definition 1. *A Laman graph is a connected graph $G = (V, E)$ with $|E| = 2|V| - 3$ and $|E(W)| \leq 2|W| - 3$ for all $W \subset V$.*

Laman graphs admit a *Henneberg construction*: an ordering $v_1, \ldots, v_n$ of the vertices such that, if G_i is the graph induced $v_1, \ldots, v_i$, then G_3 is a triangle and G_i is obtained from G_{i-1} by one of the following operations:

- (**H$_1$**) Choose two vertices x, y from G_{i-1} and add v_i together with the edges (v_i, x) and (v_i, y).
- (**H$_2$**) Choose an edge (x, y) and a third vertex z from G_{i-1}, remove (x, y) and add v_i together with the three edges (v_i, x), (v_i, y), and (v_i, z).

Planar Laman graphs also admit a *planar Henneberg construction* [16]. That is, the graph can be constructed together with a plane straight-line embedding, with each vertex remaining in the position it is inserted. The two operations of a (planar) Henneberg construction are illustrated in Figure 1.

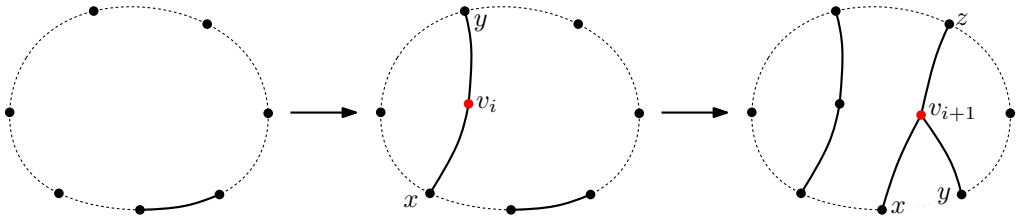

Fig. 1. Two operations of a planar Henneberg construction: an **H$_1$**-operation followed by an **H$_2$**-operation.

Let G be a planar Laman graph. From the fact that Laman graphs have $2|V| - 3$ edges easily follows that G contains a facial triangle. We choose an embedding of G in which such a triangle $\{v_1, v_2, v_3\}$ is the outer face. We can assume that the outer face remains intact during a Henneberg construction, i.e., we never perform an **H$_2$**-operation on an edge on the outer face. Let v_1, v_2, v_3 appear in this counterclockwise order around the outer triangle. We call v_1, v_2 the *special vertices* and the outer edge $e^* = (v_1, v_2)$ the *special edge* of G.

In the remainder of this section we describe three new combinatorial structures on 2-connected plane graphs. Although we define the structures for general 2-connected plane graphs, the most important structures (angular trees and edge labelings) exist only for plane Laman graphs.

2.1 Angular Structure

The *angular graph* A_G of a plane graph G is a plane bipartite graph defined as follows. The vertices of A_G are the vertices $V(G)$ and faces $F(G)$ of G and there exists an edge (v, f) between $v \in V(G)$ and $f \in F(G)$ if and only if v is incident to f. If G is 2-connected, then A_G is a maximal bipartite planar graph and every face of A_G is a quadrangle.

Definition 2. *An* angular structure *of a 2-connected plane graph G with special edge $e^* = (v_1, v_2)$ is a set T of edges of A_G with the following two properties:*

Vertex rule: *Every vertex $v \in V(G) \setminus \{v_1, v_2\}$ has exactly 2 incident edges in T. Special vertices have no incident edge in T.*
Face rule: *Every face $f \in F(G)$ has exactly 2 incident edges not in T.*

Let S be the set of edges of A_G that are not in T. The angular structure T can be represented by orienting the edges of A_G as follows. Every edge (v, f) is oriented from v to f if $(v, f) \in T$, and from f to v if $(v, f) \in S$. This way every vertex of A_G has exactly two outgoing edges (except for the special vertices). Such orientations of a maximal bipartite planar graph are called *2-orientations* and have been introduced by de Fraysseix and Ossona de Mendez [7]. It is also possible to derive an angular structure of G from a 2-orientation of A_G.

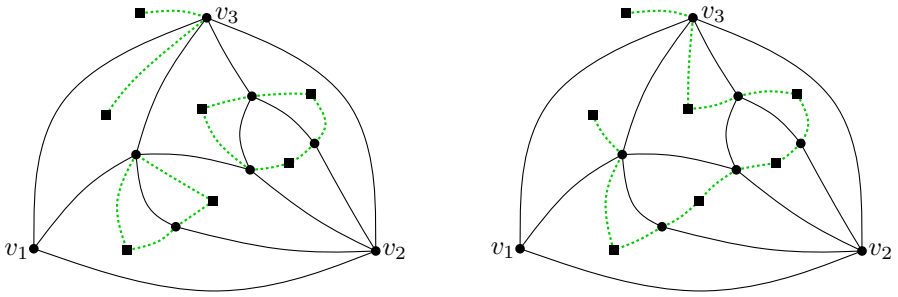

Fig. 2. Two angular structures of the same plane Laman graph. The one on the right is an angular tree.

Lemma 1 ([7]). *Every maximal bipartite planar graph has a 2-orientation. Thus every 2-connected plane graph has an angular structure.*

If G is a Laman graph, then $|F(G)| = |V(G)| - 1$ by Euler's formula. Thus every angular structure T consists of exactly $2|V(G)| - 4$ edges and spans exactly $|V(A_G)| - 2 = 2|V(G)| - 3$ vertices. Hence, if T is connected, then T is a spanning tree of $V(A_G) \setminus \{v_1, v_2\}$. An angular structure that is a tree is called an *angular tree*. In Figure 2 two angular structures of the same plane Laman graph are shown – one being an angular tree.

Next we show that every plane Laman graph admits an angular tree. Our proof is constructive and computes an angular tree along a planar Henneberg sequence of G. Consider a cycle C in A_G such that the edges of C are alternatingly in S and T. We say that C is an *alternating cycle*. We can perform a *flip* on C by removing all edges in $C \cap T$ from T and adding all edges in $C \cap S$ to T. The resulting set of edges satisfies the properties of an angular structure. A flip corresponds to reversing the edges of a directed cycle in the corresponding 2-orientation.

Lemma 2. *Let T consist of two connected components A and B, where A is a tree and B contains a cycle. If we perform a flip on an alternating 4-cycle C that contains an edge of A and an edge of the cycle in B, then the resulting angular structure is a tree.*

Proof. If we remove the edges in $C \cap T$ from T, then B becomes a tree, and we split up A into two trees A_1 and A_2. The edges in $C \cap S$ connect A_1 to B and A_2 to B. The resulting angular structure is connected and hence a tree. □

Theorem 1. *Every plane Laman graph G admits an angular tree T and it can be computed in $\mathcal{O}(|V(G)|^2)$ time.*

Proof. We build G and T simultaneously along a planar Henneberg construction, which can be found in $\mathcal{O}(|V(G)|^2)$ time using an algorithm of Bereg [2]. T remains a tree during the construction. We begin with the triangle $\{v_1, v_2, v_3\}$ and T containing the two edges incident to v_3 in A_G. Now assume we insert a vertex v into a face f of G, which is split into two faces f_1 and f_2.

For an $\mathbf{H_1}$-operation, let x and y be the original vertices of the graph. We add an edge (u, f_1) to T if and only if u is incident to f_1 and $(u, f) \in T$ before the operation. We do the same for f_2. Furthermore, we add edges (v, f_1) and (v, f_2) to T. If $(x, f) \in T$ before the operation, then we remove either (x, f_1) or (x, f_2) from T. Similarly, if $(y, f) \in T$ before the operation, then we remove either (y, f_1) or (y, f_2) from T. By choosing these edges correctly, we can ensure that f_1 and f_2 satisfy the degree constraints; see Fig. 3(left). This operation cannot introduce a cycle, so T must remain a tree.

For an $\mathbf{H_2}$-operation, let (x, y) and z be the edge and vertex of the operation. Furthermore, let f' be the face of G that shares the edge (x, y) with f before the operation. We add an edge (u, f_1) to T if and only if u is incident to f_1 and $(u, f) \in T$ before the operation (same for f_2). Furthermore, we add edges (v, f') and either (v, f_1) or (v, f_2) to T. If $(z, f) \in T$ before the operation, then we remove either (z, f_1) or (z, f_2) from T. As above, we can choose the edges to ensure that f_1 and f_2 satisfy the degree constraints. However, this operation can introduce a cycle in T containing the new vertex v (if not, we are done). Assume w.l.o.g. that f_1 is part of this cycle, and hence $(v, f_1) \in T$; see Fig. 3(right).

If $(z, f_2) \in T$, then $(z, f_1) \notin T$, and the cycle formed by (z, f_1), (z, f_2), (v, f_2), and (v, f_1) is alternating and satisfies the requirements of Lemma 2. We can flip this cycle to turn T into a tree. If $(z, f_2) \notin T$, then

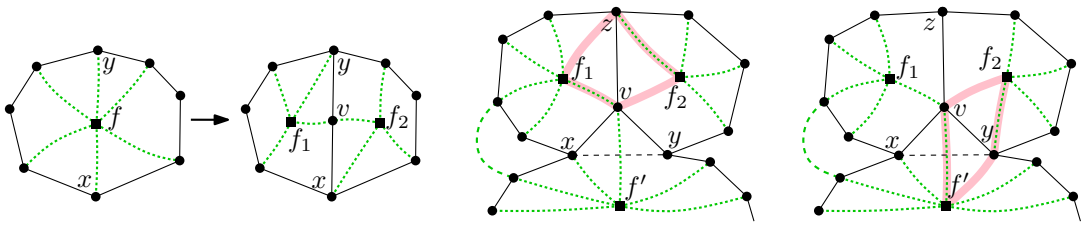

Fig. 3. Left: updating T (drawn dotted) for ($\mathbf{H_1}$). Right: alternating cycles after ($\mathbf{H_2}$).

$(y, f_2) \in T$ by the degree constraints on f_2. Also, $(y, f') \notin T$, for otherwise T would contain a cycle before the operation. Thus, the cycle formed by (y, f_2), (y, f'), (v, f'), and (v, f_2) is alternating and satisfies the requirements of Lemma 2. As before, we can flip this cycle to turn T into a tree.

At each step in the above procedure one vertex is added to G. The operations carried out to maintain the angular tree can be performed in $\mathcal{O}(1)$ time for an $\mathbf{H_1}$-operation and in $\mathcal{O}(|V(G)|)$ time for an $\mathbf{H_2}$-operation. Indeed, the bottleneck in the latter case is identifying the unique cycle in the intermediate angular structure. Thus the total runtime is $\mathcal{O}(|V(G)|^2)$, which concludes the proof. □

The following result is important for the construction of an L-contact representation of a plane Laman graph.

Lemma 3. *If T is an angular tree and f is a triangular face of G, then T contains a perfect matching between non-special vertices of G and faces of G different from f.*

Proof. Remove the vertex corresponding to f (leaf in T) from T and let v be the non-special vertex with $(v, f) \in T$. Direct all edges of T towards v. Now every face $f' \neq f$ has exactly one outgoing edge in T and every non-special vertex has exactly one incoming edge in T. The desired matching can be obtained by matching each face different from f to the unique endpoint $v \in V(G)$ of its outgoing edge in T. □

2.2 Angle Labeling

Next we define a labeling of the angles of G, using the angular structure above; see Fig. 4. This labeling for 2-connected plane graphs is similar to the Schnyder angle labeling for maximally plane graphs.

Definition 3. *An* angle labeling *of a 2-connected plane graph G with special edge $e^* = (v_1, v_2)$ is a labeling of the angles of G by $1, 2, 3, 4$, with the following two properties:*

Vertex rule: *Around every vertex $v \neq v_1, v_2$, in clockwise order, we get the following sequence of angles: exactly one angle labeled 3, zero or more angles labeled 2, exactly one angle labeled 4, zero or more angles labeled 1. All angles at v_1 are labeled 1, all angles at v_2 are labeled 2.*

Face rule: *Around every face, in clockwise order, we get the following sequence of angles: exactly one angle labeled 1, zero or more angles labeled 3, exactly one angle labeled 2, zero or more angles labeled 4.*

Theorem 2. *Every 2-connected plane graph admits an angle labeling.*

Proof. By Lemma 1 every 2-connected plane graph G admits an angular structure, which corresponds to a 2-orientation of the angular graph A_G. The edges of a 2-orientation can be colored in red and blue, such that the edges around each vertex v are ordered as follows: one outgoing red edge, zero or more incoming red edges, one outgoing blue edge, zero or more incoming blue edges (the order is clockwise for $v \in V(G)$ and counterclockwise for $v \in F(G)$). Such an orientation and coloring of the edges of a maximal bipartite planar graph is called a *separating decomposition* [7].

We now label each angle at a vertex v of G based on the color and orientation of the corresponding edge (v, f) in the separating decomposition. If the edge is incoming at v and colored blue, we label the angle 1. If the edge is incoming at v and colored red, we label the angle 2. If the edge is outgoing at v and colored red, we label the angle 3. If the edge is outgoing at v and colored blue, we label the angle 4. It is now straightforward to verify that the vertex rule and face rule are implied by the order in which incident edges appear around each vertex in the separating decomposition. □

Note that the correspondence derived above between an angular structure T and an angle labeling of G is such that $(v, f) \in T$ if and only if the corresponding angle label is 3 or 4. Moreover, from an angle labeling one can derive the corresponding separating decomposition of A_G and hence the corresponding angular structure. In particular, there is a bijection between angular structures of G and angle labelings of G.

2.3 Edge Labeling

Finally, we define an orientation and coloring of the edges of a 2-connected plane graph G based on an angular tree T of G; see Fig. 4. This edge labeling for 2-connected plane graphs is similar to the Schnyder edge labeling for maximally plane graphs.

Definition 4. *An* edge labeling *of a 2-connected plane graph G with special edge $e^* = (v_1, v_2)$ is an orientation and coloring of the non-special edges of G with colors 1 (red) and 2 (blue), such that each of the following holds:*

Vertex rule: *Around every vertex $v \neq v_1, v_2$, in clockwise order, we get the following sequence of edges: exactly one outgoing red edge, zero or more incoming blue edges, zero or more incoming red edges, exactly one outgoing blue edge, zero or more incoming red edges, and zero or more incoming blue edges. All non-special edges at v_1 are incoming and red, all non-special edges at v_2 are incoming and blue.*

Face rule: *For every inner face f there are two distinguished vertices r and b. Every red edge on f is directed from b towards r, and every blue edge is directed from r towards b. The vertices r and b are called the red and blue sink of f, respectively.*

We denote the edge labeling by (E_r, E_b), where E_r and E_b is the set of all red and blue edges, respectively.

In an edge labeling (E_r, E_b) of G every non-special vertex has two outgoing edges. Together with the special edge this makes $2|V(G)| - 3$ edges in total. Thus $|E(G)| = 2|V(G)| - 3$ and $|F(G)| = |V(G)| - 1$. Every inner face has exactly two sinks, which makes $2|F(G)| = |E(G)| - 1$ in total. Indeed, there is a one-to-one correspondence between the non-special edges of G and sinks of inner faces in (E_r, E_b). We associate every directed edge e with the inner face f incident to it as illustrated in Fig. 4(d). This way we have the following for every edge labeling (E_r, E_b) of G.

Edge rule: Every non-special edge e corresponds to one incident inner face f, such that the endpoint of e is a sink of f in the color of e.

Theorem 3. *If a 2-connected plane graph admits an angular tree, then it admits an edge labeling.*

Proof. Let G be a 2-connected plane graph and T be an angular structure of G. By Theorem 2, G admits an angle labeling that corresponds to T, i.e., the angle of a face f at a vertex v is labeled 3 or 4 if and only if $(v, f) \in T$. We split every vertex v in G, except for v_1 and v_2, into two vertices v^1 and v^2, in such a way that for $i = 1, 2$ all edges incident to an angle labeled i are incident to v^i. We call the resulting graph H. In other words H arises from G by splitting each non-special vertex along its two edges in T. Thus, as T is acyclic, H is connected. Since H consists of $2|V(G)| - 2$ vertices (v_1, v_2 plus $2(|V(G)| - 2)$ split vertices) and $|E(G)| = 2|V(G)| - 3$ edges, H is a tree.

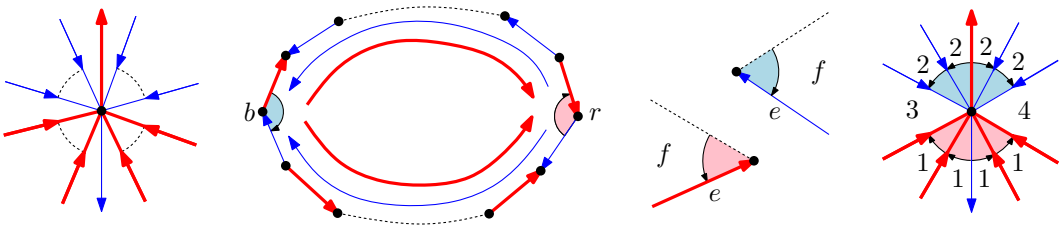

Fig. 4. Vertex rule (a), face rule (b), and edge rule (c)-(d). Red edges are drawn thick.

We orient every edge e in H towards the special edge e^* of G. We color e red if it is outgoing at some v^2 and blue if it is outgoing at some v^1. It is now straightforward to check, using the vertex rule and face rule of the angle labeling, that this orientation and coloring of all non-special edges is indeed a valid edge labeling of G. □

Not every edge labeling corresponds to an angular tree. Furthermore, some but not all angular structures that are not trees correspond to an edge labeling. For example, the angular structure in Figure 2 (left) does not have a corresponding edge labeling. Hence, edge labelings of G and angular structures (or angular trees) of G are *not* in bijection.

Theorem 4. *An edge labeling (E_r, E_b) of a 2-connected plane graph G with special edge $e^* = (v_1, v_2)$ has the following two properties:*

(i) The graph $E_r \cup E_b^{-1}$ ($E_b \cup E_r^{-1}$) is acyclic, where E_b^{-1} is E_b with the direction of all edges reversed.
(ii) The graph E_r (E_b) is a spanning tree of $G \setminus \{v_2\}$ ($G \setminus \{v_1\}$) with all edges directed towards v_1 (v_2).

Proof. Consider the graph $E_r \cup E_b^{-1}$. Since every vertex except for v_1 and v_2 has an outgoing red edge and an outgoing blue edge, there is only one source (all edges are outgoing at v_2) and one sink (all edges are incoming at v_1) in $E_r \cup E_b^{-1}$. By the face rule, every face has exactly one source (the blue sink) and one sink (the red sink). The face rule for the inner face of G containing the special edge e^* implies that the outer cycle as well has exactly one source (v_1) and exactly one sink (v_2). Every nesting minimal (the set of faces it circumscribes is inclusion minimal) directed cycle in a plane graph is either a facial cycle or has a source or sink in its interior. This proves (i). Part (ii) follows directly from part (i) and the fact that every non-special vertex has one outgoing edge in E_r (E_b). □

3 L-Contact Graphs

An *L-shape* $\mathcal{L}$ is a path consisting of exactly one horizontal segment and exactly one vertical segment. There are four different types of L-shapes; see Fig. 5(left). Two L-shapes $\mathcal{L}_1$ and $\mathcal{L}_2$ make *contact* if and only if the endpoint of one of the two L-shapes coincides with an interior point of the other L-shape; see Fig. 5(middle). If the endpoint belongs to $\mathcal{L}_1$, then we say that $\mathcal{L}_1$ makes contact with $\mathcal{L}_2$. Note that we do not allow contact using the bend of an L-shape; see Fig. 5(right).

A graph $G = (V, E)$ is an *L-contact graph* if there exist non-crossing L-shapes $\mathcal{L}(v)$ for each $v \in V$, such that $\mathcal{L}(u)$ and $\mathcal{L}(v)$ make contact if and only if $(u, v) \in E$. We call these L-shapes the *L-contact representation* of G. We can match edges of L-contact graphs to endpoints of L-shapes. However, an endpoint that is bottommost, topmost, leftmost, or rightmost cannot correspond to an edge. We call an L-contact representation *maximal* if every endpoint that is neither bottommost, topmost, leftmost, nor rightmost makes a contact, and there are at most three endpoints that do not make a contact. We assume that the bottommost, topmost, leftmost, and rightmost endpoints are uniquely defined.

In a maximal L-contact representation of a graph G, each inner face of G is bounded by a simple rectilinear polygon, which is contained in the union of all L-shapes. Now each $\mathcal{L}(v)$ has a right angle, which is a convex corner of the polygon corresponding to one incident face at v and a concave corner corresponding to another incident face at v, provided the corresponding face is an inner face.

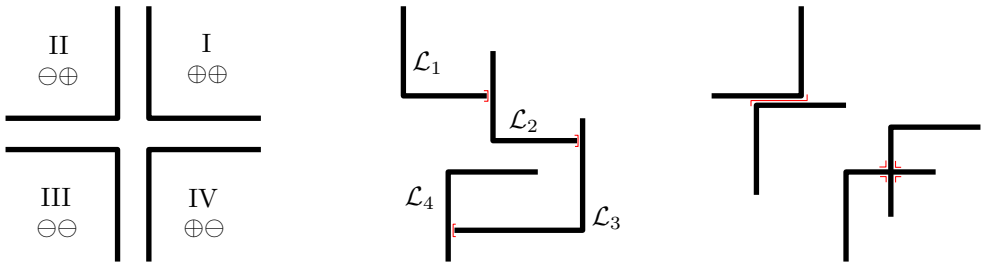

Fig. 5. Left: possible L-shapes. Middle: valid contacts. Right: invalid contacts.

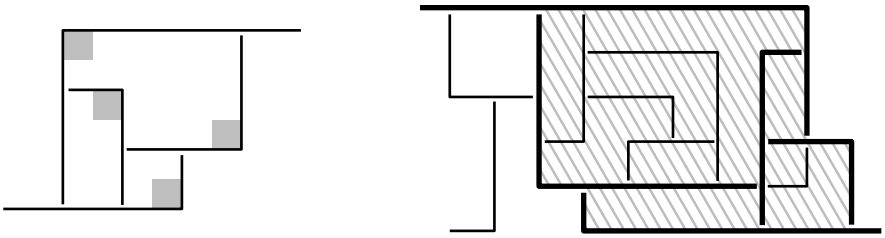

Fig. 6. Left: K_4 is an L-contact graph but not a Laman graph. Right: Illustration of the proof of Lemma 4.

Lemma 4. *If a graph G has a maximal L-contact representation in which each inner face contains the right angle of exactly one $\mathcal{L}$, then G is a plane Laman graph.*

Proof. Consider a maximal L-contact representation of G in which every inner face contains the right angle of exactly one $\mathcal{L}$. By the definition of maximal L-contact representations, we get that $|E(G)| \geq 2|V(G)| - 3$. We need to show that $|E(W)| \leq 2|W| - 3$ for all subsets $W \subseteq V(G)$ of at least two vertices. For the sake of contradiction, let W be a set ($|W| \geq 2$) with $|E(W)| \geq 2|W| - 2$. It follows that at most two endpoints of L-shapes corresponding to vertices in W do not make contact when restricted to W. Since this holds for one bottommost endpoint and one topmost endpoint, we have $|E(W)| = 2|W| - 2$. Moreover, if we choose W to be inclusion-minimal among all such sets, then $G(W)$ is 2-connected; see thick L-shapes corresponding to W in Fig. 6.

The outer face of $G(W)$ is bounded by a rectilinear polygon $\mathcal{P}$ with two additional ends sticking out. This polygon is highlighted in Fig. 6. Consider the vertex set $W' \supseteq W$ of all vertices whose corresponding L-shapes are contained in $\mathcal{P}$, i.e., $G(W)$ is a subgraph of $G(W')$ and every inner face of $G(W')$ is an inner face of G. Since the representation is maximal we have $|E(W')| = |E(W)| + 2|W' \setminus W| = 2|W'| - 2$. Hence $G(W')$ has too many edges as well. We want to show that one inner face of $G(W')$ has two convex angles, which would then complete the proof.

Let k be the number of outer vertices of $G(W')$. Since $\mathcal{P}$ has only two endpoints sticking out, all but two of its convex corners are due to a single $\mathcal{L}$, i.e.,

$$\#\text{convex corners of } \mathcal{P} \leq k + 2.$$

Each outer edge of $G(W')$, except for two, corresponds to a contact that is a concave corner of $\mathcal{P}$, i.e.,

$$\#\text{concave corners of } \mathcal{P} \geq k - 2.$$

In every rectilinear polygon the number of concave corners is exactly the number of its convex corners minus four. Thus we conclude that both inequalities above must hold with equality. In particular, every concave corner of $\mathcal{P}$ corresponds to a contact of two L-shapes and no concave corner is due to a single $\mathcal{L}$. Moreover, every L-shape corresponding to an outer vertex in $G(W')$ forms a convex corner of $\mathcal{P}$. Hence for every $w \in W'$ the right angle of $\mathcal{L}(w)$ lies inside $\mathcal{P}$.

By Euler's formula $G(W')$ has precisely $|W'| - 1$ inner faces. Since there are $|W'|$ right angles among those inner faces, one inner face must have two right angles. □

Definition 5. *A maximal L-contact representation is* proper *if every inner face contains the right angle of exactly one $\mathcal{L}$. An L-contact graph is* proper *if it has a proper L-contact representation.*

Lemma 4 states that all proper L-contact graphs are plane Laman graphs. The main result of the remainder of this section is the following.

Theorem 5. *Plane Laman graphs are precisely proper L-contact graphs.*

To obtain an L-contact representation of a plane Laman graph, we require only the existence of an angular tree with the corresponding edge labeling. Thus, if a 2-connected plane graph G admits an angular tree, then it has a corresponding edge labeling by Theorem 3, and we can compute a proper L-contact representation of G. We obtain the following characterization of planar Laman graphs as a by-product of our approach.

Theorem 6. *A planar 2-connected graph is a Laman graph if and only if it admits an angular tree.*

3.1 Vertex Types

Assume we have an angular tree T with corresponding edge labeling (E_r, E_b) for a plane Laman graph G. Every non-special vertex v in G has two incident edges in T. The other endpoint of such an edge corresponds to a face in G. These are the two faces that contain the bend of $\mathcal{L}(v)$. The matching M of T obtained from Lemma 3 (using the outer face of G as the triangular face) determines for every vertex of G the incident inner face f containing the right angle of $\mathcal{L}(v)$. The outgoing red (blue) edge of a vertex v determines the contact made by the horizontal (vertical) leg of $\mathcal{L}(v)$.

We derive from M and (E_r, E_b) the type of the L-shape $\mathcal{L}(v)$ for every vertex v. The *red sign* and *blue sign* of a vertex v, denoted by $t_r(v)$ and $t_b(v)$, represent the direction of the horizontal and vertical leg of $\mathcal{L}(v)$, respectively. We write the type of v as $t(v) = t_r(v)t_b(v)$, or as its quadrant number (see Fig. 5 left).

First we set $t_b(v_1) = \oplus$ and $t_r(v_2) = \oplus$ (the red sign of v_1 and the blue sign of v_2 are irrelevant). For every non-special vertex v, let $e_r(v)$ ($e_b(v)$) be its outgoing red (blue) edge, and $e_M(v)$ its incident edge in M. The angle between $e_r(v)$ and $e_b(v)$ that contains $e_M(v)$ is called the *matched angle*. The opposite angle is called the *unmatched angle* (v_1 and v_2 have only an unmatched angle). We set the types according to the following rule.

Type rule: Let $e = (u, v)$ be a directed edge from u to v of color c. If e lies in the unmatched angle of v, we set $t_c(u) = t_c(v)$, otherwise $t_c(u) \neq t_c(v)$.

We need to check if this type rule, along with T, M, and (E_r, E_b), results in a correct L-contact representation. Around every vertex v, the neighboring vertices with incoming edges to v must have the correct red or blue sign. For example, if $t(v) = \text{I}$ and the edge $u \to v$ is blue and lies in the matched angle of v, then $t_b(u) = \ominus$. Note that this follows directly from the type rule (see Fig. 7 left).

Secondly, the convex angle of an L-shape $\mathcal{L}(v)$ must belong to the face that contains $e_M(v)$. For example, if $e_b(v), e_M(v), e_r(v)$ appear in clockwise order around v, then $t(v) = \text{I}$ or $t(v) = \text{III}$. We say v is *odd* if $e_b(v), e_M(v), e_r(v)$ appear in clockwise order around v, and *even* otherwise.

Lemma 5. *A non-special vertex v is odd if and only if $t_r(v) = t_b(v)$.*

Proof. Consider the directed red path P_1 from v to v_1 and the directed blue path P_2 from v to v_2 (see Fig. 7 middle). Since $E_r \cup E_b^{-1}$ is acyclic by Theorem 4, $P_1 \cap P_2$ consists only of v. Let C be the cycle formed by P_1, P_2 and the special edge e^*, and G' be the maximal subgraph of G whose outer cycle is C. We define r_1, r_2, r_3, r_4 as follows (we define b_1, b_2, b_3, b_4 analogously w.r.t. P_2):

$$r_1 := \#\{e = (u, v) \in P_1 \mid e \text{ in unmatched angle of } v \text{ and } e_M(v) \text{ outside } G'\}$$
$$r_2 := \#\{e = (u, v) \in P_1 \mid e \text{ in unmatched angle of } v \text{ and } e_M(v) \text{ inside } G'\}$$
$$r_3 := \#\{e = (u, v) \in P_1 \mid e \text{ in matched angle of } v \text{ and } e_M(v) \text{ outside } G'\}$$
$$r_4 := \#\{e = (u, v) \in P_1 \mid e \text{ in matched angle of } v \text{ and } e_M(v) \text{ inside } G'\}$$

Now let $k = |C|$ be the number of vertices on C and $|V(G')| = k + n'$. Then G' has $2n' + k + r_2 + r_3 + b_2 + b_3$ edges and thus by Euler's formula $n' + b_2 + b_3 + r_2 + r_3 + 1$ inner faces. On the other hand $G' \setminus \{v\}$ contains exactly $n' + b_2 + b_4 + r_2 + r_4$ matching edges. So if v is odd, then e_M lies inside G', too. Since the number of inner faces and matching edges must coincide we have $b_3 + r_3 = b_4 + r_4$. In particular $b_3 + b_4$ and $r_3 + r_4$ have the same parity, which means that the red and blue sign of v coincide. If v is even, then e_M lies outside G' and we get $b_3 + r_3 + 1 = b_4 + r_4$, which implies that $b_3 + b_4$ and $r_3 + r_4$ have different parity. Hence the red sign and blue sign at v are distinct. □

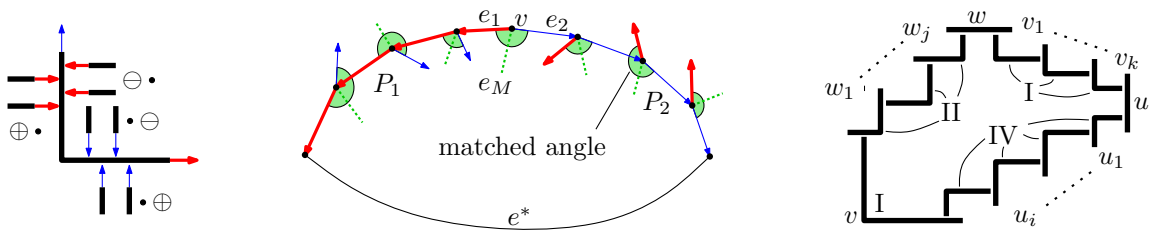

Fig. 7. Left/Right: types around a vertex/face ($t(v) = \text{I}$). Middle: proof Lemma 5.

Finally we consider the faces in the L-contact representation. Every inner face f of G has three special vertices: the two sinks u and w, as well as the vertex v that f is matched to in M. Let $u, u_1, \ldots, u_i, v, w_1, \ldots, w_j, w$, $v_1, \ldots, v_k$ be the clockwise order of the vertices around f. The type rule implies the following shape of faces in the L-contact representation (see Fig. 7 right).

Lemma 6. *Let v be the vertex that is matched to a face f, and t be the type of v. Then we have the following:*

- *Each of $u_1, \ldots, u_i$ has type $t-1$.*
- *Each of $v_1, \ldots, v_k$ has type t.*
- *Each of $w_1, \ldots, w_j$ has type $t+1$.*

3.2 Inequalities

Given the type of every vertex v, it suffices to find the point $(x(v), y(v)) \in \mathbb{R}^2$ where the bend of $\mathcal{L}(v)$ is located. Additionally we define for each inner face f an auxiliary point $(x(f), y(f)) \in \mathbb{R}^2$, which in the L-contact representation of G will correspond to some point in the bounded region corresponding to f.

We use two directed (multi-)graphs D_r and D_b on the vertices and inner faces of G to describe inequalities for the x- and y-coordinates, respectively. For every inequality $x(u) < x(v)$ ($y(u) < y(v)$) there is an edge $u \to v$ in D_r (D_b), where $u, v \in V(G) \cup F(G)$. Both graphs D_r and D_b contain all edges of G. The direction of an edge (u, v) can be determined by $t(u)$, $t(v)$, and (E_r, E_b). An edge $u \to v$ is in D_r iff (i) $u \to v \in E_r$ and $t_r(u) = \oplus$, (ii) $v \to u \in E_r$ and $t_r(v) = \ominus$, (iii) $u \to v \in E_b$ and $t_r(v) = \ominus$, or (iv) $v \to u \in E_b$ and $t_r(u) = \oplus$. Similarly, $u \to v$ is in D_b iff (i) $u \to v \in E_b$ and $t_b(u) = \oplus$, (ii) $v \to u \in E_b$ and $t_b(v) = \ominus$, (iii) $u \to v \in E_r$ and $t_b(v) = \ominus$, or (iv) $v \to u \in E_r$ and $t_b(u) = \oplus$.

We need to ensure that the L-contact representation is non-crossing. The inequalities above are not sufficient to achieve this. Therefore we add additional inequalities for each inner face. These inequalities ensure that each inner face does not cross itself in the L-contact representation. The inequalities for each type of face are shown in Table 1. Figure 8 illustrates the directed edges of D_r and D_b around a face of G. See Appendix B for more details.

	$t(v) = \oplus\oplus$	$t(v) = \ominus\oplus$	$t(v) = \ominus\ominus$	$t(v) = \oplus\ominus$
D_r	$w_j \to f; f \to v_1, u_i$	$v_k, w_1 \to f; f \to u_1$	$v_1, u_i \to f; f \to w_j$	$u_1 \to f; f \to w_1, v_k$
D_b	$u_1 \to f; f \to w_1, v_k$	$w_j \to f; f \to v_1, u_i$	$v_k, w_1 \to f; f \to u_1$	$v_1, u_i \to f; f \to w_j$

Table 1. The three inequality edges of a face f of G in D_r and D_b for each type of f.

The following lemma is straightforward yet tedious to prove, and hence the proof is relegated to the appendix.

Lemma 7. *The graphs D_r and D_b are acyclic.*

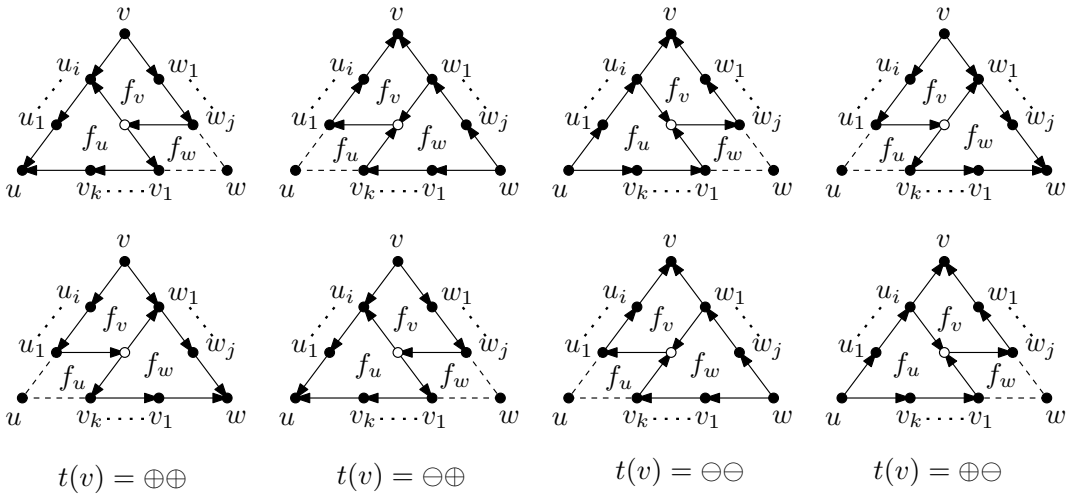

Fig. 8. The directed graphs D_r (top row) and D_b (bottom row) locally around an inner face f of G. The directions of dashed edges depend on the types of the endpoints.

3.3 Construction

Given a planar Laman graph G, an L-contact representation of G is constructed as follows:

(1) Find a planar Henneberg construction for G.
(2) Compute an angular tree T of G (Theorem 1).
(3) Compute the angle and edge labeling of G w.r.t. T (Theorem 2 and 3).
(4) Compute the type of every vertex of G according to the type rule in Section 3.1. This can be computed using a simple traversal of the trees E_r and E_b.
(5) Define the directed graphs D_r and D_b as described in Section 3.2
(6) Compute a topological order of D_r and D_b and let, for every vertex v in G, $x(v)$ and $y(v)$ be the number of v in these topological orders, respectively.
(7) For every non-special vertex v with $v \to u$ in E_r and $v \to w$ in E_b define an L-shape $\mathcal{L}(v)$ whose horizontal leg spans from $x(v)$ to $x(u)$ on y-coordinate $y(v)$ and whose vertical leg spans from $y(v)$ to $y(w)$ on x-coordinate $x(v)$.

Let n be the number of vertices of G. By Theorem 1 we can compute an angular tree of G in $\mathcal{O}(n^2)$ time. The angle labeling w.r.t. T can be computed in $\mathcal{O}(n)$ time using the linear time algorithm of de Fraysseix and Ossona de Mendez [7]. Similarly, the edge labeling w.r.t. T can be computed by a simple traversal of the tree H described in the proof of Theorem 3. It is easy to see that the remaining steps of our algorithm can also be computed in $\mathcal{O}(n)$ time. Finally note that the vertices of D_r and D_b that correspond to inner faces of G do not need to be included in the topological order of D_r and D_b. Hence every coordinate used in the L-contact representation is between 1 and n.

Theorem 7. *The algorithm above computes an L-contact representation of G on an $n \times n$ grid in $\mathcal{O}(n^2)$ time, where n is the number of vertices of G. If an angular tree is given, then the algorithm runs in $\mathcal{O}(n)$ time.*

4 Future Work and Open Problems

Using our newly discovered combinatorial structure, we showed that planar Laman graphs are L-contact graphs. Thus, we showed that axis-aligned L's are as "powerful" as segments with arbitrary slopes when it comes to *contact representation of planar graphs* [1]. The equivalent result is not true for *intersection representation of planar graphs*. Indeed there is no k such that all segment intersection graphs have an intersection representation with axis-aligned paths with no more than k bends each [3].

We think that L-contact representations can be used in various settings. For example, by "fattening" the L's we can get proportional side-contact representations similar to those in [1].

Several natural open problems follow from our results:

1. There are L-contact graphs that are not Laman graphs (e.g. K_4). All L-contact graphs are planar and satisfy $|E(W)| \leq 2|W| - 2$ for all $W \subseteq V$. Are these conditions also sufficient?
2. The L-contact representations resulting from our algorithm use all four types of L-shapes. If we limit ourselves to only type-I L's we can represent planar graphs of tree-width at most 2, which include outerplanar graphs. What happens if we limit ourselves to only type-I L's **and** allow degenerate L's?
3. Not every edge labeling corresponds to an angular tree. What are the necessary conditions for an edge labeling to have a corresponding (not necessarily proper) L-contact representation?
4. Planar Laman graphs can be characterized by the existence of an angular tree, which we can compute in $\mathcal{O}(n^2)$ time. This is slower than the fastest known algorithm for recognizing Laman graphs, which runs in $\mathcal{O}(n^{3/2}\sqrt{\log n})$ time [5]. Can we compute angular trees faster, as to obtain a faster algorithm for recognizing planar Laman graphs?

Acknowledgments. The research in this paper started during the *Bertinoro Workshop on Graph Drawing*. The authors gratefully acknowledge the other participants for useful discussions.

References

1. M. J. Alam, T. Biedl, S. Felsner, M. Kaufmann, and S. G. Kobourov. Proportional contact representations of planar graphs. In *Proc. 19th Symposium on Graph Drawing*, pages 26–38, 2011.
2. S. Bereg. Certifying and constructing minimally rigid graphs in the plane. In *Proc. 21st Symposium on Computational Geometry*, pages 73–80. 2005.
3. S. Chaplick, V. Jelínek, J. Kratochvíl, and T. Vyskočil. Bend-bounded path intersection graphs: Sausages, noodles, and waffles on a grill. In *Proc. 38th International Workshop on Graph Theoretic Concepts in Computer Science*. 2012.
4. J. Czyzowicz, E. Kranakis, and J. Urrutia. A simple proof of the representation of bipartite planar graphs as the contact graphs of orthogonal straight line segments. *Information Processing Letters*, 66(3):125–126, 1998.
5. O. Daescu and A. Kurdia. Towards an optimal algorithm for recognizing laman graphs. *Journal of Graph Algorithms and Applications*, 13(2):219–232, 2009.
6. N. de Castro, F. J. Cobos, J. C. Dana, A. Márquez, and M. Noy. Triangle-free planar graphs and segment intersection graphs. *Journal of Graph Algorithms and Applications*, 6(1):7–26, 2002.
7. H. de Fraysseix and P. Ossona de Mendez. On topological aspects of orientations. *Discrete Mathematics*, 229:57–72, 2001.
8. H. de Fraysseix and P. Ossona de Mendez. Representations by contact and intersection of segments. *Algorithmica*, 47:453–463, 2007.
9. H. de Fraysseix, P. Ossona de Mendez, and J. Pach. Representation of planar graphs by segments. *Intuitive Geometry*, 63:109–117, 1991.
10. H. de Fraysseix, P. Ossona de Mendez, and P. Rosenstiehl. On triangle contact graphs. *Combinatorics, Probability & Computing*, 3:233–246, 1994.
11. S. Felsner. Lattice structures from planar graphs. *Electronic Journal of Combinatorics*, 11:R15, 2004.
12. S. Felsner and M. C. Francis. Contact representations of planar graphs with cubes. In *Proc. 27th Symposium on Computational Geometry*, pages 315–320, 2011.
13. S. Felsner, C. Huemer, S. Kappes, and D. Orden. Binary labelings for plane quadrangulations and their relatives. *Discrete Mathematics & Theoretical Computer Science*, 12(3):115–138, 2010.
14. É. Fusy. Transversal structures on triangulations: A combinatorial study and straight-line drawings. *Discrete Mathematics*, 309(7):1870–1894, 2009.
15. J. Graver, B. Servatius, and H. Servatius. *Combinatorial Rigidity*. Grad. Stud. in Math. 2. American Math. Soc., 1993.
16. R. Haas, D. Orden, G. Rote, F. Santos, B. Servatius, H. Servatius, D. Souvaine, I. Streinu, and W. Whiteley. Planar minimally rigid graphs and pseudo-triangulations. *Computational Geometry*, 31:31–61, 2005.
17. P. Koebe. Kontaktprobleme der konformen Abbildung. *Berichte über die Verhandlungen der Sächsischen Akademie der Wissenschaften zu Leipzig. Math.-Phys. Klasse*, 88:141–164, 1936.
18. G. Laman. On graphs and rigidity of plane skeletal structures. *Journal of Engineering Mathematics*, 4:331–340, 1970.
19. P. Rosenstiehl and R. Tarjan. Rectilinear planar layouts and bipolar orientations of planar graphs. *Discrete & Computational Geometry*, 1:343–353, 1986.
20. W. Schnyder. Planar graphs and poset dimension. *Order*, 5(4):323–343, 1989.
21. W. Schnyder. Embedding planar graphs on the grid. In *Proc. 1st ACM-SIAM Symposium on Discrete Algorithms*, pages 138–148, 1990.

A Example

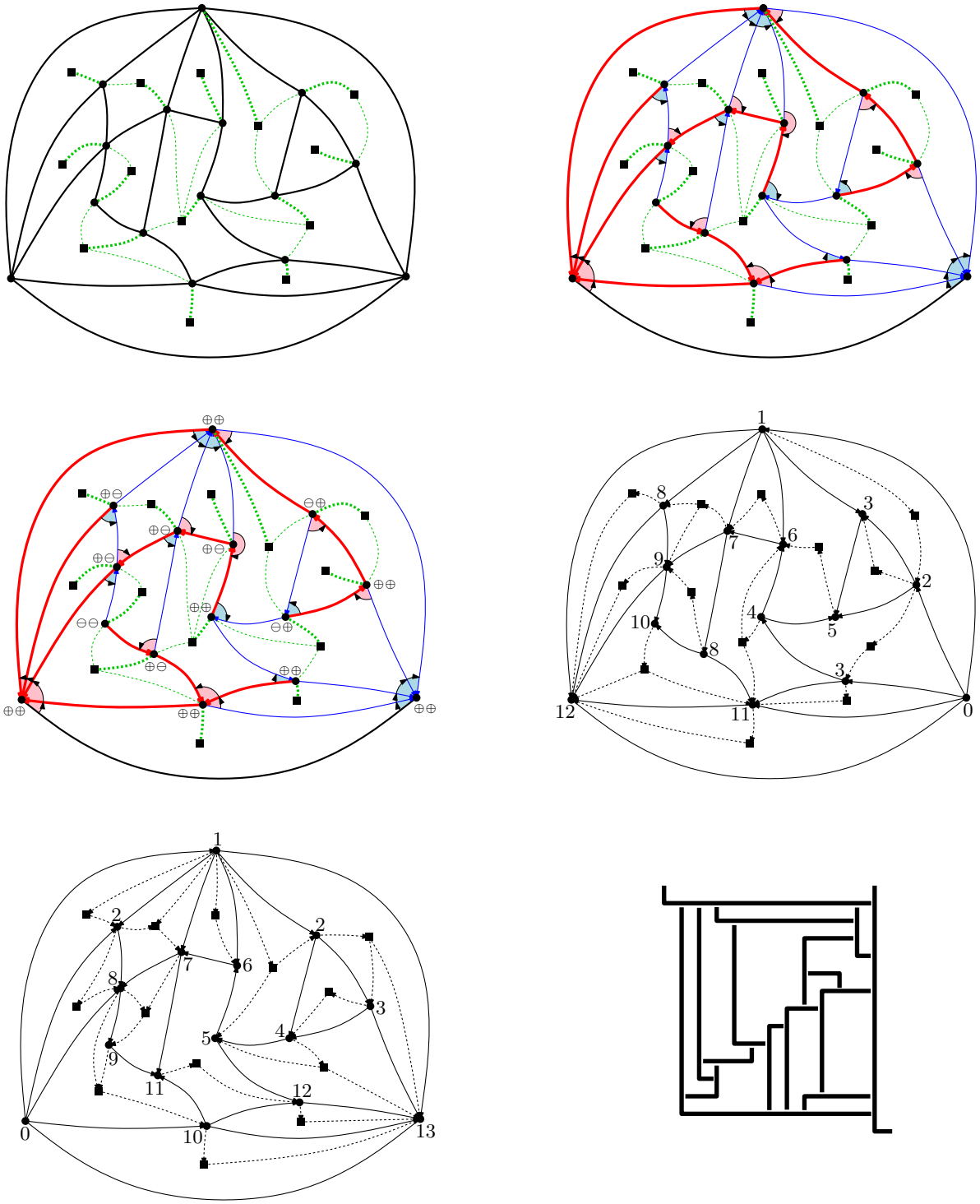

Fig. 9. Left top: angular tree, and the corresponding matching (thick). Right top: edge labeling corresponding to angular tree. Middle left: vertex types. Middle right: inequality graph D_r plus x-coordinates. Bottom left: inequality graph D_b plus y-coordinates. Bottom right: L-contact representation.

B Inequality graphs

We begin by defining how an edge (u, v) of G is directed in D_r and D_b. An edge $u \to v$ is in D_r if and only if (i) $u \to v \in E_r$ and $t_r(u) = \oplus$, (ii) $v \to u \in E_r$ and $t_r(v) = \ominus$, (iii) $u \to v \in E_b$ and $t_r(v) = \ominus$, or (iv) $v \to u \in E_b$ and $t_r(u) = \oplus$. Similarly, $u \to v$ is in D_b if and only if (i) $u \to v \in E_b$ and $t_b(u) = \oplus$, (ii) $v \to u \in E_b$ and $t_b(v) = \ominus$, (iii) $u \to v \in E_r$ and $t_b(v) = \ominus$, or (iv) $v \to u \in E_r$ and $t_b(u) = \oplus$.

The special edge $e^* = (v_1, v_2)$ is directed $v_2 \to v_1$ in D_r and $v_1 \to v_2$ in D_b. Note that this is consistent with the above rules using $t_b(v_1) = \oplus = t_r(v_2)$ and putting either $v_1 \to v_2$ into E_b or $v_2 \to v_1$ into E_r.

We can derive from the face rule of the edge labeling (E_r, E_b), the types around a face (Lemma 6), and the definition of directed edges above, how the edges of a face f of the Laman graph G are oriented in D_r and D_b. We remark that some edges of D_r, D_b, namely those between faces and vertices of G, are yet to be defined, and that a facial cycle in G will correspond to a non-facial cycle in D_r, as well as D_b.

Let f be an inner face in G with its three distinguished vertices u, v, w. For convenience we put $u_{i+1} = v = w_0$, $w_{j+1} = w = v_0$, and $v_{k+1} = u = u_0$. Then all but two edges of f appear in D_r and D_b according to the following table:

	$t(v) = \oplus\oplus$	$t(v) = \ominus\oplus$	$t(v) = \ominus\ominus$	$t(v) = \oplus\ominus$
D_r	$u_0 \leftarrow \ldots \leftarrow u_{i+1}$ $v_1 \rightarrow \ldots \rightarrow v_{k+1}$ $w_0 \rightarrow \ldots \rightarrow w_j$	$u_1 \rightarrow \ldots \rightarrow u_{i+1}$ $v_0 \rightarrow \ldots \rightarrow v_k$ $w_0 \leftarrow \ldots \leftarrow w_{j+1}$	$u_0 \rightarrow \ldots \rightarrow u_{i+1}$ $v_1 \leftarrow \ldots \leftarrow v_{k+1}$ $w_0 \leftarrow \ldots \leftarrow w_j$	$u_1 \leftarrow \ldots \leftarrow u_{i+1}$ $v_0 \leftarrow \ldots \leftarrow v_k$ $w_0 \rightarrow \ldots \rightarrow w_{j+1}$
D_b	$u_1 \leftarrow \ldots \leftarrow u_{i+1}$ $v_0 \leftarrow \ldots \leftarrow v_k$ $w_0 \rightarrow \ldots \rightarrow w_{j+1}$	$u_0 \leftarrow \ldots \leftarrow u_{i+1}$ $v_1 \rightarrow \ldots \rightarrow v_{k+1}$ $w_0 \rightarrow \ldots \rightarrow w_j$	$u_1 \rightarrow \ldots \rightarrow u_{i+1}$ $v_0 \rightarrow \ldots \rightarrow v_k$ $w_0 \leftarrow \ldots \leftarrow w_{j+1}$	$u_0 \rightarrow \ldots \rightarrow u_{i+1}$ $v_1 \leftarrow \ldots \leftarrow v_{k+1}$ $w_0 \leftarrow \ldots \leftarrow w_j$

Table 2. The edges of a face f of G (except for two) form in D_r and D_b three directed paths.

The situation around a face f is illustrated in Figure 10. The two edges e, e' in f that are not listed for D_r (D_b) in Table 2 are incident to the blue (red) sink of f. These are the dashed edges in the figure.

Lemma 8. *The two edges incident to the blue (red) sink s of f are directed in D_r (D_b) both incoming at s if $t_r(s) = \ominus$ ($t_b(s) = \ominus$) and both outgoing at s if $t_r(s) = \oplus$ ($t_b(s) = \oplus$).*

Proof. If both edges e and e' are incoming at the blue (red) sink s in the edge labeling, then they are colored blue (red). By definition e and e' are incoming at s in D_r (D_b) if and only if the red (blue) sign of s is $\ominus$.

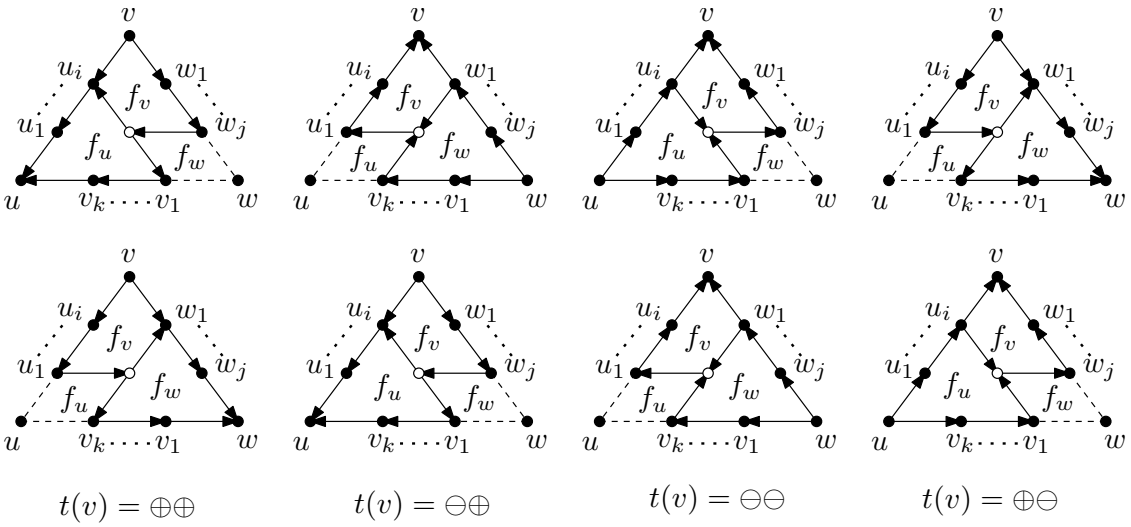

Fig. 10. The directed graphs D_r (top row) and D_b (bottom row) locally around an inner face f of G. The directions of dashed edges depend on the types of the endpoints.

If in the edge labeling e is incoming at s while e' is outgoing, then e is blue (red) and e' is red (blue). (Note that by the face rule e and e' can not be both outgoing at a sink of that face.) Again e and e' are incoming at s in D_r (D_b) iff the red (blue) sign of the end-vertex of e, which is s, and the start-vertex of e', which is s as well, is $\ominus$. □

Next we define the remaining edges in D_r and D_b, i.e., those that join a vertex with an inner face of G. Consider an inner face f with its three distinguished vertices u, v, w. If $t(v) = \oplus\oplus$ then we have in D_r the edges $w_j \to f, f \to v_1$ and $f \to u_i$, and in D_b the edges $u_1 \to f, f \to v_k$ and $f \to w_1$. If $t(v) = \ominus\oplus$ then we have in D_r the edges $v_k \to f, f \to u_1$ and $w_1 \to f$, and in D_b the edges $w_j \to f, f \to v_1$ and $f \to u_i$. If $t(v) = \ominus\ominus$ then we have in D_r the edges $u_i \to f, v_1 \to f$ and $f \to w_j$, and in D_b the edges $w_1 \to f, v_k \to f$ and $f \to u_1$. If $t(v) = \oplus\ominus$ then we have in D_r the edges $u_1 \to f, f \to v_k$ and $f \to w_1$, and in D_b the edges $u_i \to f, v_1 \to f$ and $f \to w_j$. We again refer to Figure 10 for an illustration.

In case any of $u_1, u_i, v_1, v_k, w_1, w_j$ does not exist, we replace it in the above definition as follows: Replace v_1/u_i by u, u_1/w_j by v, and v_k/w_1 by w. This may introduce parallel edges, e.g., when $t(v) = \oplus\oplus$ and neither v_1 nor u_i exists.

Lemma 7. *The graphs D_r and D_b are acyclic.*

Proof. First note that D_r and D_b are planar. More precisely, either graph inherits a plane embedding from G by putting a vertex for each inner face f into the corresponding bounded region and connecting it by three edges to some of its incident vertices. This way f is divided into three inner faces f_u, f_v, f_w, each corresponding to a different distinguished vertex of f, that is u, v, w are incident to f_u, f_v, f_w, respectively. See Figure 10 for an illustration.

To prove that D_r is acyclic, it now suffices to show that every inner face of D_r is acyclic, the special vertex v_2 is the only vertex with only outgoing edges and v_1 is the only vertex with only incoming edges. Similarly we want to show that every inner face of D_b is acyclic, v_1 is the unique source in D_b, and v_2 the unique sink.

Let us consider only D_r, since an analogous argumentation holds for D_b. Every inner face of D_r is one of the three faces f_u, f_v, f_w that correspond to an inner face f of G. We consider f, its three distinguished vertices u, v, w and assume w.l.o.g. that $t(v) = \oplus\oplus$. The cases that $t(v) \in \{\ominus\oplus, \ominus\ominus, \oplus\ominus\}$ are similar. We want to show that each of f_u, f_v, f_w is acyclic, i.e., contains a vertex whose two incident edges in that face are either both incoming or both outgoing:

(i) The face f_u contains the edges $f \to u_i$ (or $f \to u$) and $f \to v_1$ (or $f \to u$)[4] In particular, both edges at the vertex f are outgoing and thus f_u is acyclic.
(ii) The face f_w is a quadrangle consisting of the vertices w, v_1 (or u), f, and w_j (or v). The two edges incident to w are its two edges in the face f of G. Thus by Lemma 8 f_w is acyclic.
(iii) The face f_v contains the edges $f \to u_i$ and $v \to u_i$ if u_i exists, and the edges $f \to u$ and $v \to u$ if u_i does not exist. Thus both edges at u_i or u are incoming, and f_v is acyclic.

It remains to show that every vertex different from v_1, v_2 has at least one incoming and one outgoing edge in D_r. This is true by definition for vertices that correspond to inner faces of G. For every inner vertex v of G consider the inner face f of G such that (v, f) is in the angular structure but not in the angular matching M. This means that v is in the set $\{u_1, \ldots, u_i, v_1, \ldots, v_k, w_1, \ldots, w_j\}$ with respect to the face f. Now Table 2 and the definition of the three edges in D_r incident to f imply that v has one incoming and one outgoing edge locally around the face f. Finally, by definition we have $v_2 \to v_3$ and $v_3 \to v_1$ in D_r, which concludes the proof. □

Recall that, by the edge rule of the edge labeling (see Section 2.3), every non-special edge $u \to v$ is associated with one of its incident faces, such that v is a sink of this face. Let B_1, B_2, R_1, R_2 be the four blocks of incoming blue and red edges at v, where B_1, $e_r(v)$, B_2, R_1, $e_b(v)$, R_2 appear around v in this clockwise circular order. As illustrated in Figure 4(d), each face within R_1 and B_1 is associated with the counterclockwise next incident edge and each face within R_2 and B_2 with the clockwise next incident edge.

[4] If neither u_i nor v_1 exists, then f_u consists only of two parallel edges directed from f to u.

Lemma 9. *Let $u \to v$ be a blue (red) edge and f be the face associated with it. Then D_r (D_b) contains the edge $u \to f$ if $t_r(v) = \oplus$ ($t_b(v) = \oplus$) and the edge $f \to u$ if $t_r(v) = \ominus$ ($t_b(v) = \ominus$).*

Proof. We prove the statement only for a blue edge $u \to v$, i.e., v is the blue sink of the face f. The argument for red edges is analogous.

Consider the red sign of v and the blue sign of u. From the type rule follows that $t_r(v) \neq t_b(u)$ if $u \to v \in B_1$ and $t_r(v) = t_b(u)$ if $u \to v \in B_2$. Indeed, if v is odd, i.e., $t_r(v) = t_b(v)$, then $u \to v$ lies in B_1 if and only if $u \to v$ lies in the matched angle of v, which is the case if and only if $t_b(u) \neq t_b(v) = t_r(v)$. Similarly, if v is even, i.e., $t_r(v) \neq t_b(v)$, then $u \to v$ lies in B_1 if and only if $u \to v$ lies in the *un*matched angle of v, which is the case if and only if $t_b(u) = t_b(v) \neq t_r(v)$.

If w denotes the vertex that the face f is matched to, then from Lemma 6 follows $t_b(w) = t_b(u)$. If $t_b(w) = \oplus$ (and hence $t_r(v) = \ominus$), then the edges in D_r between vertices and faces of G are directed counterclockwise around the blue sink of f (which is v). Now by the edge rule of the edge labeling (see Section 2.3), u comes counterclockwise before v on f if and only if $u \to v$ lies in B_2. Thus we have the edge $u \to f$ in D_r iff $u \to v \in B_2$, which is the case iff $t_r(v) = t_b(u) = \ominus$.

Figure 11 shows how some edges around v are directed in D_b.

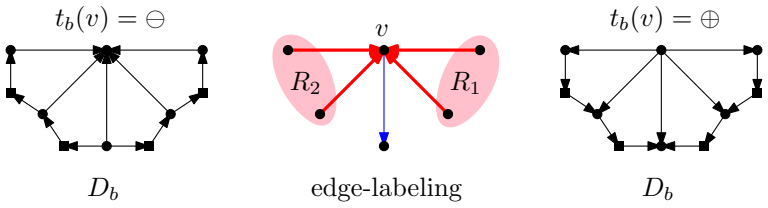

Fig. 11. The inequality graph D_b around a vertex v.

□

C Omitted Proofs

Lemma 6. *Let v be the vertex that is matched to a face f, and t be the type of v. Then we have the following:*

- *Each of $u_1, \ldots, u_i$ has type $t - 1$.*
- *Each of $v_1, \ldots, v_k$ has type t.*
- *Each of $w_1, \ldots, w_j$ has type $t + 1$.*

Proof. Let us assume that v is odd, i.e., e_r, e_M, e_b appear around v in this counterclockwise order. (The case that v is even is analogous.) Then the face rule and vertex rule imply that v, the blue sink of f, and the red sink of f appear around f in this clockwise order, i.e., u and w are the red and blue sink of f, respectively. Every vertex incident to f, except for u, v, w, has an edge with f in the angular tree T but not in the matching M. This means that f lies in the unmatched angle of each such vertex. Together with the face rule of the edge labeling, this implies that $u_1, \ldots, u_i$ and $w_1, \ldots, w_j$ are even, while $v_1, \ldots, v_k$ are odd.

Consider the edge e between v and w_1. If e is blue, then it is directed from v to w_1 and lies in the unmatched angle of w_1. Hence $t_b(w_1) = t_b(v)$. Since w_1 is even, its type is indeed $t + 1$. If e is red, then it is directed from w_1 to v and lies in the matched angle of v. Hence $t_r(w_1) \neq t_r(v)$. Again, since w_1 is even, its type is $t + 1$. Every edge between w_l and w_{l+1} ($l < i$) lies in the unmatched angle of its endpoint and hence both vertices have the same red or blue sign. Since both are even, they have in fact the same type. Similarly, one can show that each of $u_1, \ldots, u_i$ has type $t - 1$.

Now consider $w = v_0, v_1, \ldots, v_k, v_{k+1} = u$. Again all edges among those vertices that end at v_l ($1 \leq l \leq k$) lie in the unmatched angle of their endpoint. Hence since $v_1, \ldots, v_k$ are all odd, they have the same type (either t or $t + 2$). For w, the blue sink of f, we have three cases. If both edges at w are incoming (and hence blue), then both lie in the same angle (either matched or unmatched) of w and thus $t_b(v_1) = t_b(w_j)$, which implies $t(v_1) = t(v)$. If $w \to v_1$ is red and $w_j \to w$ is incoming blue and lies in the matched angle of w, then w is even.

It follows that $t_b(w_j) \neq t_b(w)$ and $t_r(w_j) \neq t_r(w) = t_r(v_1)$. This again implies $t(v_1) = t(v)$. If $w_j \to w$ lies in the unmatched angle of w, then w is odd and we have $t_b(w_j) = t_b(w) = t_r(w) = t_r(v_1) = t_b(v_1)$ as desired. Similarly, if $w \to w_j$ is red and $v_1 \to w$ lies in the matched angle of w, then w is odd and $t_r(w) = t_r(w_j)$, $t_b(w) \neq t_b(w_j)$, and $t_b(w) \neq t_b(v_1)$. Thus $t_b(w_j) = t_b(v_1)$, which implies $t(v_1) = t(v)$. Finally if $v_1 \to w$ lies in the unmatched angle of w, then w is even and we have $t(w_j) = t(w)$, and $t_b(w_j) = t_b(w) = t_b(v_1)$ as desired. □

Theorem 7. *The algorithm above computes an L-contact representation of G on an $n \times n$ grid in $\mathcal{O}(n^2)$ time, where n is the number of vertices of G. If an angular tree is given, then the algorithm runs in $\mathcal{O}(n)$ time.*

Proof. The running time of the algorithm and the size of the drawing have already been argued in Section 3.3. It remains to show that the constructed L-shapes indeed form an L-contact representation of G. First note that an L-shape $\mathcal{L}(v)$ is of type t if and only if the corresponding vertex has type t. To see this, consider a non-special vertex v of G with $t_r(v) = \oplus$. Let u be its outgoing red neighbor in the edge labeling, that is, in E_r we have the edge $v \to u$. By definition (case (i)) D_r contains the edge $v \to u$ and thus $x(v) < x(u)$. This means that the vertical leg of $\mathcal{L}(u)$ lies to the right of the vertical leg of $\mathcal{L}(v)$. In particular $\mathcal{L}(v)$ is either of type I or IV, as desired. Similarly assume that $t_b(v) = \ominus$ and consider the outgoing blue neighbor w of v. Then by definition (case (ii)) D_b contains the edge $w \to v$, which implies that $\mathcal{L}(v)$ has type III or IV. Thus if $t(v) = \oplus\ominus$ then $\mathcal{L}(v)$ is of type IV. The cases $t(v) \in \{\oplus\oplus, \ominus\oplus, \ominus\ominus\}$ are similar.

The rest of the proof is divided into several claims.

Claim 1. All edges in G are represented by non-degenerate point contacts of the corresponding L-shapes.

Proof. W.l.o.g. consider a red edge $u \to v \in E_r$. The horizontal endpoint of $\mathcal{L}(u)$ is given by $(x(v), y(u))$ and the vertical leg of $\mathcal{L}(v)$ is supported by the line $x = x(v)$, but it remains to show that $(x(v), y(u))$ lies on the vertical leg of $\mathcal{L}(v)$, i.e., $y(v) < y(u) < y(w)$ or $y(v) > y(u) > y(w)$, where w is the outgoing blue neighbor of v.

If $t_b(v) = \oplus$, then by Lemma 9 there is a directed path in D_b from v via u to the outgoing blue neighbor w of v and hence $y(v) < y(u) < y(w)$. Similarly if $t_b(v) = \ominus$, then there is a directed path in D_b from w via u to v and hence $y(v) > y(u) > y(w)$, which is what we wanted to show. △ *Claim 1.*

Claim 2. Going around $\mathcal{L}(v)$ the contacts with other L-shapes appear in the same cyclic order as the incident edges of v in the plane embedding of G.

Proof. Consider the vertex v in the edge labeling and assume w.l.o.g. that $t(v) = \oplus\oplus$, i.e., $\mathcal{L}(v)$ is of type I. Recall that R_1, R_2, B_1, B_2 denote the blocks of incoming red and blue edges around v in this clockwise cyclic order. By the type rule we know that $t_b(u) = \ominus$ for each $u \to v \in B_1$, $t_b(u) = \oplus$ for each $u \to v \in B_2$, $t_r(u) = \oplus$ for each $u \to v \in R_1$, and $t_r(u) = \ominus$ for each $u \to v \in R_2$. Since the types of L-shapes match the types of the vertices they represent, we get that each $\mathcal{L}(u)$ makes contact with $\mathcal{L}(v)$ on the correct side of the correct leg of $\mathcal{L}(v)$, e.g., $\mathcal{L}(u)$ touches the vertical leg of $\mathcal{L}(v)$ from the left for $u \to v \in R_1$ and so on.

It remains to show that within each block the contacts appear in the same cyclic order as the corresponding edges in the plane embedding of G. Consider any block, say R_1, and still assume that $t_b(v) = \oplus$. Let w be the outgoing blue neighbor of v. Then by Lemma 9 there is a directed path in D_b starting at v, going through all incoming red neighbors in R_1 in clockwise order, and ending at w (see Figure 11). In other words, the y-coordinates of $\mathcal{L}(v)$, the L-shapes in R_1 in clockwise order, and $\mathcal{L}(w)$ are increasing, which is what we wanted to show.

The consideration of R_2, B_1 and B_2, as well as cases with $t_b(v) \neq \oplus$ are analogous. △ *Claim 2.*

Claim 3. Every face f of G corresponds to a rectilinear polygonal region whose boundary is contained in the L-shapes corresponding to the vertices of f.

Proof. It is easy to see that the statement holds for the outer face. So consider any inner face f and let u, v, w be its three distinguished vertices. Let us trace the polygonal path P that is the claimed boundary of the region corresponding to f. Start at the bend of $\mathcal{L}(v)$ and go along the vertical leg on its right side if v is odd and on its left side if v is even. Whenever we meet a contact we turn right for v odd and left for v even, and traverse the other L-shape on the corresponding side. From Claim 2 follows that P is a closed path (corresponding to the inner face f).

The type of each vertex of f (except for u and w) is given by Lemma 6. Moreover, each such vertex has an edge with f in the angular structure, which means that the bend of the corresponding L-shape is on P. Finally, from Table 2 and Figure 8 we see that P is divided into three monotone parts, P_{vw} between $\mathcal{L}(v)$ and $\mathcal{L}(w)$, P_{wu} between $\mathcal{L}(w)$ and $\mathcal{L}(u)$, and P_{uv} between $\mathcal{L}(u)$ and $\mathcal{L}(v)$. So the only thing that could happen is that P_{vw} intersects P_{uv} as illustrated in the left of Figure 12.

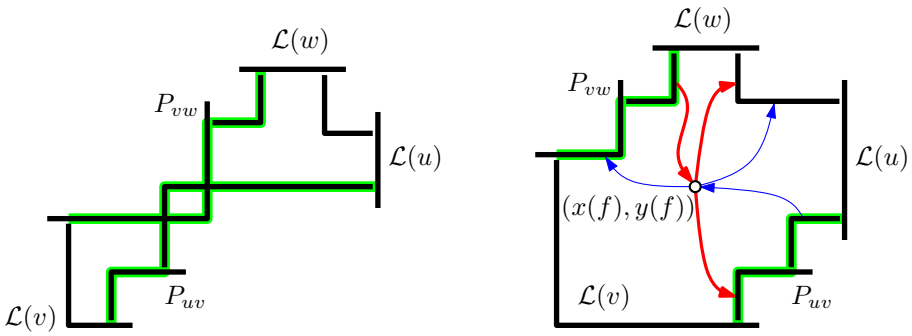

Fig. 12. Left: A situation where P_{vw} and P_{uv} intersect. Right: The introduction of the point $(x(f), y(f))$ forces P_{vw} and P_{uv} to be disjoint.

Recall that we introduced a point $(x(f), y(f)) \in \mathbb{R}^2$ associated with the face f. We claim that this point ensures that P is non-crossing. Consider for example the case that $\mathcal{L}(v)$ has type I. If $P_{vw} \cap P_{uv} \neq \emptyset$ then $x(w_j) > x(u_i)$ and $y(u_1) > y(w_1)$. But by definition we have a path $w_j \to f \to u_i$ in D_r and a path $u_1 \to f \to w_1$ in D_b (see Figure 12 right). Thus $x(w_j) < x(f) < x(u_i)$ and $y(u_1) < y(f) < y(w_1)$, which means that P is indeed not self-intersecting and thus proves the claim. $\triangle$ *Claim 3.*

Next, we consider the embedding of G inherited from the touching L-shapes (vertices are placed inside the corresponding L and edges are drawn along the L-shapes through the corresponding touching point.). By Claim 2 this embedding has the correct rotation scheme and by Claim 3 every face is crossing-free. Since G is 2-connected it follows that this embedding is the plane embedding of G we started with. In particular no two L-shapes cross each other. This completes the proof. $\square$